Pharm Res (2015) 32:1931–1946
DOI 10.1007/s11095-014-1587-9

RESEARCH PAPER

Pharmacokinetic/Pharmacodynamic Modeling of Renin-Angiotensin Aldosterone Biomarkers Following Angiotensin-Converting Enzyme (ACE) Inhibition Therapy with Benazepril in Dogs

Jonathan P. Mochel • Martin Fink • Mathieu Peyrou • Antoine Soubret • Jérôme M. Giraudel • Meindert Danhof

Received: 22 July 2014 / Accepted: 24 November 2014 / Published online: 2 December 2014

ABSTRACT

Purpose The objective of this research was to provide a comprehensive description of the effect of benazepril on the dynamics of the renin-angiotensin aldosterone system (RAAS) in dogs.

Methods Blood specimens for renin activity (RA), angiotensin II (AII), and aldosterone (ALD) quantitation in plasma were drawn from 12 healthy adult beagle dogs randomly allocated to 2 treatment groups: (i) benazepril 5 mg PO, q24 h (n: 6) and (ii) placebo (n: 6), in a cross-over design. A mechanism-based pharmacokinetic/pharmacodynamic model, which includes the periodic nature of RA, AII, and ALD during placebo treatment and the subsequent changes in dynamics following repeated dosing with benazepril, was developed.

Results The disposition kinetics of benazepril active metabolite, benazeprilat, was characterized using a saturable binding model to the angiotensin converting enzyme. The modulatory effect of benazeprilat on the RAAS was described using a combination of immediate response models. Our data show that benazepril noticeably influences the dynamics of the renin cascade, resulting in a substantial decrease in AII and ALD, while increasing RA throughout the observation span.

Conclusions The model provides a quantitative framework for better understanding the effect of ACE inhibition on the dynamics of the systemic RAAS in dogs.

KEY WORDS benazeprilat · mechanism-based PK/PD · RAAS

ABBREVIATIONS

ACE	Angiotensin-converting enzyme
AII	Angiotensin II
ALD	Aldosterone
ARA	Aldosterone receptor antagonist
ARB	Angiotensin II receptor blocker
BSV	Between-subject variability (standard deviation of the random effect)
CHF	Congestive heart failure
CV%	Coefficient of variation (%)
CVHD	Chronic valvular heart disease
EIA	Enzyme immunoassay
MB	Mechanism-based
OFV	Objective function value
PD	Pharmacodynamic
PK	Pharmacokinetics
PO	*Per os*
RA	Renin activity
RAAS	Renin-angiotensin-aldosterone system
RSE	Relative standard error (equivalent to CV%)
SD	Standard deviation
TMDD	Target-mediated drug disposition
WRES	Weighted residuals

Electronic supplementary material The online version of this article (doi:10.1007/s11095-014-1587-9) contains supplementary material, which is available to authorized users.

J. P. Mochel • M. Danhof
Department of Pharmacology, Leiden-Academic Centre for Drug Research 2300 Leiden, The Netherlands

J. P. Mochel (✉) • M. Fink • A. Soubret
Department of Integrated Quantitative Sciences, Novartis Campus St. Johann WSJ-27.6.023, 4002 Basel, Switzerland
e-mail: jonathan.mochel@novartis.com

M. Peyrou
Department of Therapeutics Research, Novartis Centre de Recherche Sante Animale SA 1566 St-Aubin, Switzerland

J. M. Giraudel
Department of Research and Development, Novartis Werk Rosental 4058 Basel, Switzerland

NOTATIONS

C_{ij}	ng/ml, or nmol/l (nM) Predicted total benazeprilat concentration at time t_{ij} for an individual *i*
Δ_{ij}	pg/ml Predicted difference between AII concentrations during placebo treatment and those at corresponding times t_{ij} after benazepril administration for an individual *i*
T_{inf}	h Duration of the hypothetical infusion of benazepril into the depot compartment
ka	h^{-1} First-order rate constant representing the absorption of benazepril into the central compartment and its *in vivo* conversion to benazeprilat
k_{10}	h^{-1} First-order rate constant of benazeprilat elimination from the central compartment
k_1	$nM^{-1}.h^{-1}$ Second-order rate constant of association of the benazeprilat-ACE complex
k_2	h^{-1} First-order rate constant of dissociation of the benazeprilat-ACE complex
BS	nM Maximal binding capacity to circulating ACE
V_c/F	l/kg Apparent volume of distribution of benazeprilat
Cl/F	$l.h^{-1}$/kg Apparent systemic clearance of benazeprilat
E	− Global extraction coefficient of benazeprilat
M	pg/ml or $pg/ml.h^{-1}$ Mesor (daily average of rhythm)
A	pg/ml or $pg/ml.h^{-1}$ Amplitude of the cosine function
ψ	h Acrophase (or time of peak) of the cosine function
τ	h Period of the cosine function
$I_{max\ (AII)}$	− Maximum inhibition of AII production
$IC_{50\ (AII)}$	ng/ml Benazeprilat concentration that produces half of the maximum inhibition of AII
$\gamma_{(AII)}$	− Hill coefficient of the AII *vs.* benazeprilat effect curve
$E_{max\ (RA)}$	− Maximum stimulatory effect on RA
$EC_{50\ (RA)}$	pg/ml Difference in AII between placebo and benazepril-treated dogs for achieving 50% of the maximal stimulation of RA
$\gamma_{(RA)}$	− Hill coefficient of the RA *vs.* AII effect curve
$I_{max\ (AL\ D)}$	− Maximum inhibition of ALD production
$IC_{50\ (ALD)}$	pg/ml Difference in AII between placebo and benazepril-treated dogs for achieving 50% of the maximal inhibition of ALD
$\gamma_{(ALD)}$	− Hill coefficient of the ALD *vs.* AII effect curve

INTRODUCTION

Canine congestive heart failure (CHF) most often develops consequent to chronic mitral valvular heart disease (CVHD) (1), a condition that affects about 75% of dogs over the age of 16 (2). Similar to humans, activation of systemic and tissue mediators of the renin-angiotensin aldosterone system (RAAS) plays a pivotal role in the pathophysiology of heart failure in dogs (3).

Elevated angiotensin II (AII) plasma levels have been associated with poorer prognosis and increased mortality in human patients with CHF. In a study by Roig *et al.* (4), AII concentrations were a significant predictor of death or new heart failure episodes in patients with left ventricular dysfunction. Later, Güder *et al.* (5) showed that high ALD levels were a predictor of increased mortality risk in human patients with CHF of any cause and severity. Long-term elevation of aldosterone (ALD) contributes to an exaggerated workload, inducing myocyte hypertrophy, necrosis and fibrosis (6), leading to the progression of the disease to its end stage (7).

Modulation of the RAAS by angiotensin-converting enzyme (ACE) inhibitors is associated with significant reduced mortality in human and canine patients suffering from CHF (8). Benazepril hydrochloride (Fortekor®; Novartis Animal Health, Basel, Switzerland) (PubChem CID: 5362124) is a nonsulphydryl prodrug which is converted *in vivo* into benazeprilat, a highly potent and selective inhibitor of ACE (9) with well-documented effectiveness in canine CHF (8).

According to Toutain and Lefebvre (10), an oral daily dose of 0.125 mg/kg benazepril would produce inhibition of the entire systemic ACE pool within 48 h in dogs. However, results from our previous research (11) in dogs receiving on average 0.7 mg/kg benazepril only showed partial reduction of AII after 5 days of dosing, which is consistent with earlier observations in human patients under ACE inhibition therapy (12,13). Taken together, these findings suggest that ACE activity may not be a sensitive endpoint to properly assess the modulatory effect of benazepril on the RAAS.

Despite the importance of benazepril in the management of heart diseases in canine patients, no detailed information about the relation of benazeprilat to renin activity (RA), AII, and ALD time-variations is presently available. The objective of this study was to provide a comprehensive description of the effect of benazeprilat on the dynamics of the renin-angiotensin cascade in dogs, using a nonlinear mixed-effects pharmacokinetic/

pharmacodynamic (PK/PD) modeling approach. Furthermore, similar determinants of RAAS activation (*i.e.* renal hypoperfusion) and regulation (*e.g.* interactions with the β-adrenergic system) can be found in dog and human CHF patients (3,14), and the use of ACE inhibitors is part of the standard of care therapy in both species. Therefore, information generated in dogs also further improves the understanding of the effect of ACE inhibition on the dynamics of the RAAS in humans.

MATERIALS AND METHODS

Animals

The study was performed in compliance with a registered Swiss permit covering animal experiments for Cardiovascular Research in Dogs as approved by the Cantonal Animal Welfare Committee and Novartis Veterinary Services. The study protocol was designed to use the fewest number of animals while being consistent with the scientific needs of the research, and conformed to the Principles of Laboratory Animal Care (NIH publication # 85–23, revised in 1985).

Twelve healthy adult (6 males and 6 females), non-neutered, 40–44 months old beagle dogs weighing between 11.9 and 19.3 kg (Marshall Europe, Green Hill, Montichiari, Italy) were randomly allocated to 2 treatment groups: (*i*) benazepril 5 mg PO, q24 h (n: 6) and (*ii*) placebo (*i.e.* benazepril vehicle) (n: 6), in a cross-over design. The average dosage of benazepril was 0.34 mg/kg (SD: 0.04 mg/kg).

Suitability for inclusion was evaluated by a physical examination and confirmed by analysis of diverse hematological (red and white blood cells counts, Hb, Hct) and clinical chemistry (albumin, total protein, alanine aminotransferase, aspartate aminotransferase, blood urea nitrogen, creatinine) parameters.

Housing Conditions

Dogs were acclimatized to the experimental facility at least 1 week prior to the experiment. Animals were housed in individual pens (about 2 m^2/animal) containing granulate bedding material and an additional elevated platform for resting. The study room had natural daylight and additional artificial light of similar intensity (400 lux) from 07:00 to 19:00 h. Room temperature and relative humidity were within the target ranges of 17 to 23°C and 35 to 75%, respectively. Drinking water quality was compliant with the Swiss Federal Regulation on Foodstuff, and was offered *ad libitum*. Starting 5 days before drug administration, the dogs were offered a low-sodium diet (0.05% sodium) at 13:00 h, as a noninvasive, fully reversible, and reliable model of RAAS activation in dogs (11). Depending on the size of the ration, the individual daily sodium intake ranged from 5.8 to 9.5 mEq. The amount of food given per dog was kept constant throughout the study.

Experimental Procedure

Dogs received benazepril or placebo tablets for 5 days at 07:00 h. Blood specimens for benazeprilat, RA, AII, and ALD quantitation in plasma were withdrawn from the *vena jugularis* into 1.2 or 2.7 ml S-Monovette tubes (Sarstedt Inc., Newton, NC, USA). Samples were collected after 5 days of oral dosing at the following timepoints relative to administration: −1, 0 (just before dosing), + 1, 2, 4, 6, 12, 13, and 16 h. Due to the known sensitivity of the renin-angiotensin cascade to posture and external stimuli (15), specific precautions were taken: *i*) dogs were kept and maintained in the same position (up and standing) during blood collection, *ii*) sampling was performed in a sound-protected room, and *iii*) low-intensity lighting was used during withdrawal. Blood samples were cooled on ice, and centrifuged under refrigeration (2±1°C, 15 min) within 30 min of sampling. Plasma was then transferred into cooled propylene tubes, snap-frozen, and stored at −80°C.

Analytical Methods

Benazeprilat concentrations in dog plasma were measured using a solid phase extraction and liquid chromatography-tandem mass spectrometry method. Calibration standards ranging from 0.5 to 250.0 ng/ml were used for quantification. As described by Mochel *et al.* (11,16,17), RA was determined by calculating the rate of angiotensin I (AI) formation after incubation of endogenous renin and angiotensinogen in plasma (2 h, 37°C, pH 7.2). AI concentrations were measured after liquid solid extraction using a validated enzyme immunoassay (EIA) test (S-1188 Angiotensin I-EIA kit; host: rabbit high-sensitivity European Conformity (CE)-marked; Bachem, Bubendorf, Switzerland). Analyses were performed in duplicates; values with a CV% below 25% were retained for statistical evaluation. AII plasma concentrations were analyzed using a validated EIA test with a specific monoclonal anti-AII antibody (A05880 Angiotensin II SPIE-IA kit; Bertin Pharma, Montigny le Bretonneux, France). Analyses were performed in duplicates, values with a CV% below 30% were retained for statistical evaluation. ALD concentrations were determined with a liquid chromatography-tandem mass

spectrometry method using an isotope dilution technique. Calibration standards ranging from 20 to 2000 pg/ml were used for quantification in plasma.

Data Analysis

Chi-Square Statistics for Testing the Zero-Amplitude Hypothesis

To determine the periodic nature of RA, AII, and ALD during placebo treatment, a *p*-value was derived from the difference in objective function value (OFV) between the fit of a constant mean (1 model parameter), and that of a 24-h cosine function (3 model parameters). In nonlinear mixed-effects models the OFV is derived as minus 2 times the logarithm of the likelihood of the data given the model, with a lower value indicating a better model (18). The difference in OFV between two contending hierarchical models follows an asymptotic chi-square distribution with degrees of freedom equal to the difference in the number of parameters between two models. A periodic rhythm was considered to be statistically significant for a drop in OFV superior to 5.9, for a risk level α: 0.05.

Pharmacokinetic/Pharmacodynamic Modeling

Nonlinear Mixed-Effects. Benazeprilat pharmacokinetics and time-varying changes in RA, AII, and ALD were fitted by means of nonlinear mixed-effects models, using the first order conditional estimation method with interaction of NONMEM version 6 (Icon Development Solutions, Ellicott City, Maryland, USA). Individual model parameters were obtained *post-hoc* as empirical Bayes estimates.

Similar to Sheiner and Ludden (18), mathematical models were written using the following format (Eq. 1):

$$\begin{aligned} y_{ij} &= F\left(\phi_i, t_{ij}\right) + G\left(\phi_i, t_{ij}, \beta\right)\cdot\varepsilon_{ij}, \quad j = 1, \ldots, n_i \\ \phi_i &= \mu\cdot e^{\eta i}, \quad i = 1, \ldots, N \end{aligned} \tag{1}$$

Where y_{ij} is the observed variable (*e.g.* RA) measured on the i^{th} individual at time t_{ij}, ϕ_i is the vector of individual parameters, $F(\phi_i\, t_{ij})$ is the value of that observed variable at time t_{ij} for an individual with parameters ϕ_i, and ε_{ij} is an independent random variable. The function $G(\phi_i, t_{ij}, \beta)$ is the standard deviation of the error of a given measurement at time t_{ij}. In nonlinear mixed-effects models $F(\phi_i ; t_{ij})$ is known as the *structural model* (error-free), while $G(\phi_i, t_{ij}, \beta)$ is the *residual error model* (combining unexplained variability and measurement noise). μ represents the typical value (population median) of a model parameter. The sources of variation between the individual parameters ϕ_i can be further explained by population characteristics (*i.e.* covariates) that can be included additively or proportionally to μ. The independent random variables ηi represent the unexplained difference between the value of the individual parameters ϕ_i and their median μ. The random variables ε_{ij} and η_i were assumed to be normally distributed with mean value 0 and variance-covariance matrix σ^2 and ω^2, while y_{ij} and ϕ_i were log-normally distributed.

Inclusion of Covariate Relationships. Population covariates search was performed using the stepwise covariate model building tool of Perl-speaks-NONMEM (19), with forward inclusion based on *p*: 0.05 and afterwards backward exclusion based on *p*: 0.01. Covariates of interest included bodyweight and sex.

Model Evaluation Standard goodness-of-fit diagnostics, including population and individual predictions *vs.* observations, and the distributions of weighted residuals over time were used to evaluate the performances of the final model. Graphical assessment was performed using the R-based software Xpose version 4.1 (20) in R version 2.15.1. Model selection was based on statistical significance between competing models using the OFV obtained from NONMEM, graphical evaluation and validity of parameter estimates. Residual error estimates from the mathematical models were used as supportive information for evaluation of lack of fit. Normality and independance of residuals were evaluated using histograms, quantile-quantile plots, and autocorrelation of conditional weighted residuals in Xpose version 4.1.

Model Validation *Two simulation-based diagnostics were used for validation of the final model:* i) *visual predictive checks, and* ii) *mirror plots, both options being automated in Perl-speaks-NONMEM.*

i) *Visual predictive checks*

To assess the validity of final model parameter estimates, the 80% confidence interval of the 5th, 50th, and 95th percentile calculated from 1000 Monte-Carlo simulations was overlaid to the corresponding percentiles of the raw data using Xpose version 4.1.

ii) *Mirror plots*

The mirror plots option of Perl-speaks-NONMEM was used to create 3 simulation table files. Mirror plots were provided with the intention of comparing goodness-of-fits obtained from raw observations and simulated datasets. In the absence of model misspecification, simulated data should 'mirror' the diagnostic plots obtained with the original datafile. Predictions obtained from the raw observations and the simulated datasets were then evaluated graphically using Xpose version 4.1.

RESULTS

Pharmacokinetic Modeling

Individual and average benazeprilat plasma concentrations and effect on the RAAS following multiple oral dosing of benazepril (5 mg) are presented in Figs. 1 and 2. Benazeprilat data were analyzed using the class of pharmacokinetic models developed by Lees *et al.* (21) for ACE inhibitors (Fig. 3). Similar to Toutain *et al.* (22), a saturable binding model was found to fit the data reasonably well, as shown by the standard goodness-of-fit diagnostics (Fig. 4), the individual predictions (Fig. 5), and the simulation-based validation diagnostics (Figs. 6, 7, and Supplementary Material).

The final selected model is a reduced version of the physiologically-based pharmacokinetic model developed by Picard-Hagen *et al.* (23) for description of cortisol disposition in ewes. In a nutshell, a compartmental approach was used where the total amount of benazeprilat, as measured by the bioanalytical assay, is the sum of *i*) benazeprilat specifically and reversibly bound to circulating ACE (termed A_{bound}) and *ii*) benazeprilat free of binding (referred to as A_{free}) (Fig. 3). The fraction of benazeprilat that binds to tissular ACE cannot be measured by bioanalytical assays, and was not included in the final pharmacokinetic model. The *free* fraction represents the amount of benazeprilat that is systemically cleared from the central compartment, according to the first-order rate constant k_{10} (details below). The nonlinear binding to systemic ACE according to the second-order rate constant of association k_1 is reflective of a target-mediated drug disposition (TMDD) model. Note that A_{free} actually corresponds to truly free benazeprilat and benazeprilat non-specifically bound to albumin, these 2 measures being indistinguishable from a kinetics viewpoint (22,23).

Free benazeprilat was used as the driving force for describing the processes of drug elimination, and reversible binding to soluble ACE. The model of benazeprilat disposition could be described using the following equations (Eqs. 2 to 5):

$$If\ t \leq T_{inf} : d\left(A_{depot}\right)/dt = \left(\frac{Dose_{benazepril}}{T_{inf}}\right) - ka.A_{depot} \quad (2)$$

$$If\ t > T_{inf} : d\left(A_{depot}\right)/dt = -ka.A_{depot} \quad (3)$$

$$d\left(A_{free}\right)/dt = ka.A_{depot} - k_{10}.A_{free} - k_1.A_{free}.(BS - A_{bound}) + k_2.A_{bound} \quad (4)$$

$$d(A_{bound})/dt = k_1.A_{free}.(BS - A_{bound}) - k_2.A_{bound} \quad (5)$$

A sequential zero and first-order absorption model was found to best fit the data, where T_{inf} is the duration of the hypothetical infusion into the depot compartment (h), ka is a first-order rate constant (h^{-1}) representing the absorption of benazepril into the central compartment and its *in vivo* conversion to benazeprilat (Fig. 1), and t is the time (h). k_{10} is the first-order rate constant (h^{-1}) of elimination

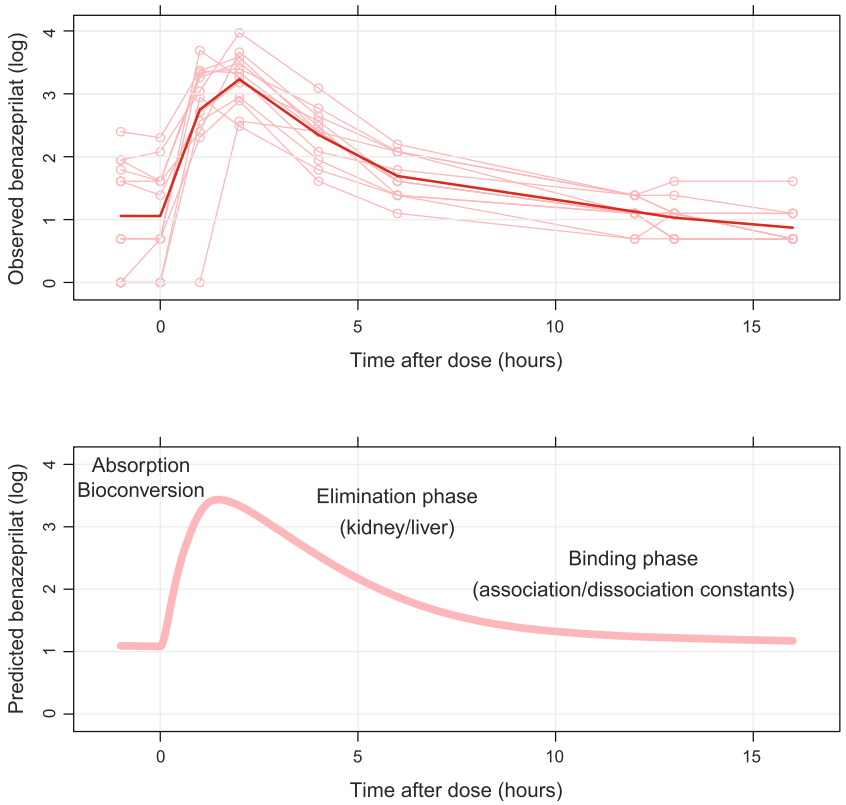

Fig. 1 Benazeprilat plasma disposition. *Top* Individual and average (*thick line*) observed benazeprilat plasma concentration *vs.* time profiles following repeated oral administrations of benazepril (5 mg PO, q24 h) in 12 healthy beagle dogs (*log scale*). *Bottom* Predicted benazeprilat disposition in a typical individual, with its physiologically-based interpretation (adapted from Toutain *et al* (22)). For ACE inhibitors, the decline of concentrations following absorption is no longer interpreted as a distribution time, but as an elimination phase controlled by the first-order rate constant k_{10}. In this representation, the terminal phase of benazeprilat disposition is driven by dissociation processes, rather than elimination from the central compartment.

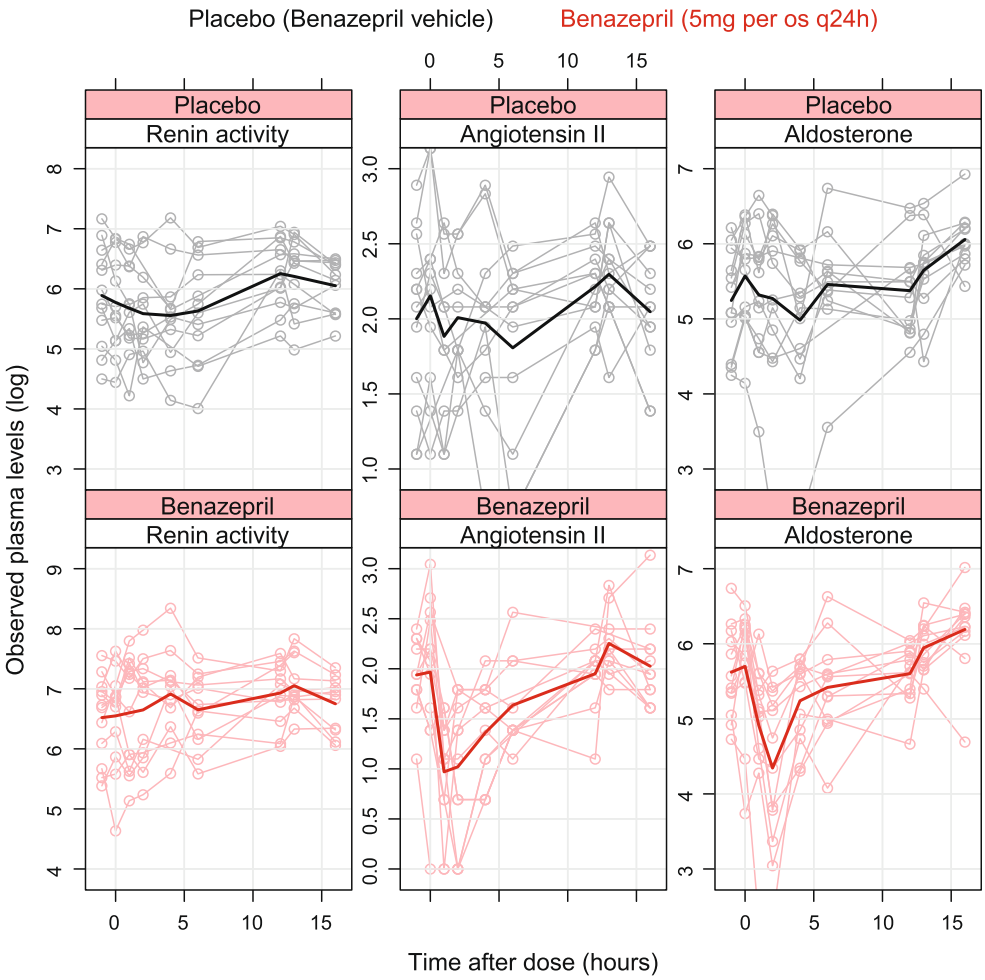

Fig. 2 Dynamics of systemic renin-angiotensin-aldosterone system (*RAAS*) peptides following repeated oral administrations of benazepril in healthy beagle dogs on a low-sodium diet. From *left* to *right*: observed individual and average (*thick line*) time-course profiles of RA, AII, and ALD in 12 dogs receiving daily placebo (*top pane*), or benazepril treatment (5 mg PO) (*bottom pane*) for 5 days in a cross-over design (*log scale*). The data support substantial differences in the dynamics of systemic RAAS peptides, resulting in a fall of AII and ALD, and a compensatory elevation of RA following ACE inhibition therapy.

from the central compartment, k_1 is the second-order rate constant ($nM^{-1}.h^{-1}$) of association of the benazeprilat-ACE complex, k_2 is the first-order rate constant (h^{-1}) of dissociation of the benazeprilat-ACE complex, and *BS* is the maximal binding capacity to circulating ACE (nM) in the central compartment. For simplification purposes the model of benazeprilat disposition was developed assuming binding to a single ACE site. A quasi-proportional error model (*i.e.* additive error in the log domain) was used to account for the residual noise in the measurement of benazeprilat.

Final estimates of the pharmacokinetic model parameters (including relative standard error, RSE and between-subject variability, BSV) are summarized in Table I. BSVs are expressed as standard deviation estimates of the random effects. The residual error (CV%) in benazeprilat predictions was estimated at 20%. The precision of the final model parameters quantified by relative standard errors was considered satisfactory (RSEs < 35%).

The estimated large apparent volume of distribution of benazeprilat (V_c/F) (6.3 l/kg) is in agreement with previous findings from Toutain *et al.* (22) in dogs. Results from the covariate analysis showed that sex, but not bodyweight, had a significant influence on V_c/F ($p<0.01$). Specifically, the apparent volume of distribution in male dogs was estimated to be 40% larger compared to females.

The apparent systemic clearance (Cl/F) of *free* benazeprilat ($l.h^{-1}/kg$) was calculated using the following relation (Eq. 6):

$$Cl/F = k_{10}.V_c \tag{6}$$

While the global extraction coefficient of benazeprilat E was derived from the estimated systemic clearance and the dog cardiac output ($ml.min^{-1}/kg$), using Eqs. 7 to 9:

$$Cardiac\ output = 180.bodyweight^{(-0.195)} \tag{7}$$

$$E = \frac{Cl/F}{Cardiac\ output} \tag{8}$$

$$E = \frac{k_{10}.V_c}{180.bodyweight^{(-0.195)}} \tag{9}$$

The apparent systemic clearance of benazeprilat was estimated to be high (3.5 $l.h^{-1}/kg$, or 58.8 $ml.min^{-1}/kg$), with a global extraction coefficient E of 0.55 for a typical 15 kg dog. Thereof, the half-life corresponding to the rate constant of

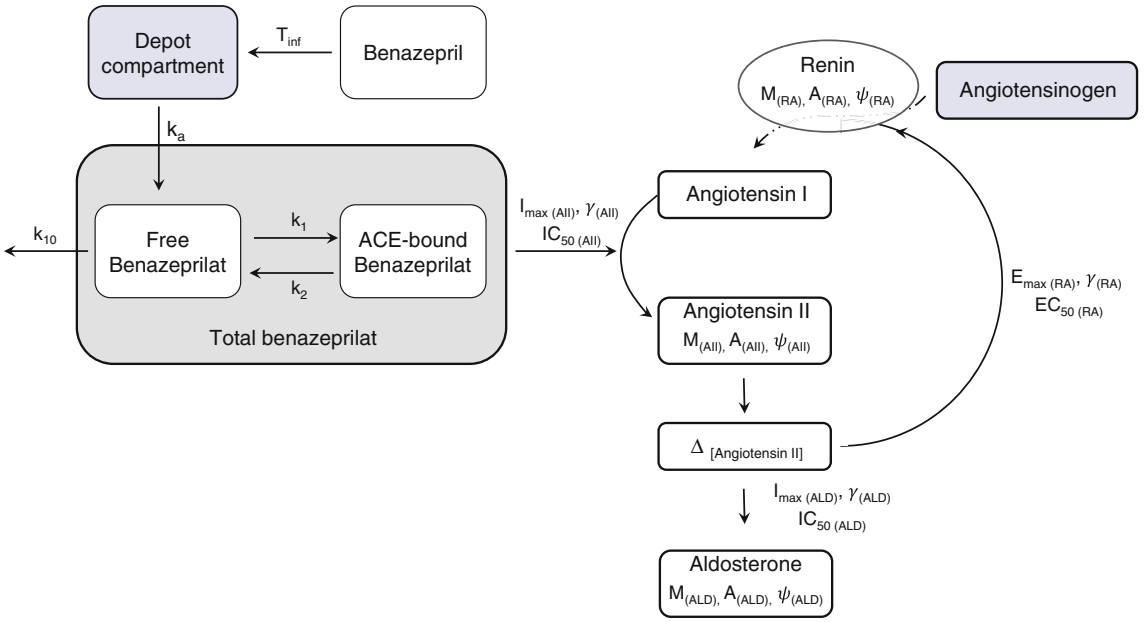

Fig. 3 Integrated pharmacokinetic/pharmacodynamic model of benazeprilat disposition and effect on the dynamics of the renin-angiotensin cascade. A stepwise integrated PK/PD model was used, which includes the chronobiology of RA, AII, and ALD during placebo treatment, and the subsequent changes in dynamics following inhibition of ACE. Benazeprilat data were analyzed using the class of pharmacokinetic models developed by Lees *et al*. (21) for ACE inhibitors. A compartmental approach was used where the total amount of benazeprilat, as measured by the bioanalytical assay, is the sum of *i*) benazeprilat specifically and reversibly bound to circulating ACE (termed A_{bound}) and *ii*) benazeprilat free of binding (referred to as A_{free}). A sequential zero and first-order absorption model was found to best fit the data, where T_{inf} is the duration of the hypothetical infusion into the depot compartment (not measured, *i.e.* shaded in *grey*), and *ka* is a first-order rate constant representing the absorption of benazepril into the central compartment and its *in vivo* conversion to benazeprilat. k_1 is the second-order rate constant of association of the benazeprilat-ACE complex, and k_2 is the first-order rate constant of dissociation of the benazeprilat-ACE complex. The *free* fraction represents the amount of benazeprilat that is systemically cleared from the central compartment, according to the first-order rate constant k_{10}. The modulatory effect of benazeprilat on the RAAS was described using a combination of immediate response models, where benazeprilat concentrations *vs*. time data served as the driving force for prediction of AII, while RA and ALD levels were derived from the predicted difference in AII during placebo and benazepril treatment. See text in Materials and Methods section for details.

elimination of *free* benazeprilat was estimated to be rather short (about 1 h). The associated high value of k_{10} (0.56 h^{-1}) compared to the rather low estimate of k_2 (0.01 h^{-1}) unveils that the terminal phase of benazeprilat disposition is driven by dissociation processes, rather than elimination from the central compartment.

Pharmacodynamic Modeling

The time-course profiles of RA, AII, and ALD in dogs receiving placebo and ACE inhibition therapy for 5 days can be found in Fig. 2. A stepwise integrated MB PK/PD model was used, which includes the periodic nature of RA, AII, and ALD during placebo treatment, and the subsequent changes in dynamics following inhibition of ACE. Typical (*i.e.* population median) parameter estimates from the pharmacokinetic model were fixed during development of the PK/PD model.

1. *Modeling of placebo data*

   The cosinor fit of the data was statistically significant for RA, AII, and ALD ($p<0.01$), supporting the hypothesis of time-varying dynamics with a 24-h period (Table II). Therefore, circadian changes in RA, AII, and ALD from the placebo data could be described according to Eq. 10:

$$f\left(t_{ij}\right) = M_i.\left(1 + A_i.cos\left(\left(t_{ij} - \psi_i\right).\left(\frac{2\pi}{\tau_i}\right)\right)\right) \qquad (10)$$

   Where $f(t_{ij})$ is the predicted RA (pg/ml.h^{-1}), AII (pg/ml), or ALD (pg/ml) placebo value at time t_{ij}, M_i is the mesor (daily average of rhythm in pg/ml, or pg/ml.h^{-1}) for the i^{th} individual, A_i is the amplitude of the cosine (pg/ml, or pg/ml.h^{-1}), ψ_i is the acrophase (or time of peak, in h), and τ_i is the fixed 24-h period of the cosine for that individual.

   Data from the various variables were fitted simultaneously, using the periodic nature of RA to estimate the acrophase and the relative amplitude of downstream biomarkers AII and ALD (the 3 endpoints sharing the same typical value). The peak RA, AII, and ALD in healthy beagle dogs fed a low-sodium diet at 13:00 h was estimated to lie around 23:00 h (Table III). Estimates of residual errors (CV%) from the mathematical models were 38%, 30%, and 50% for RA, AII, and ALD, respectively. The precision of the final model parameters was considered adequate (RSE<20%).

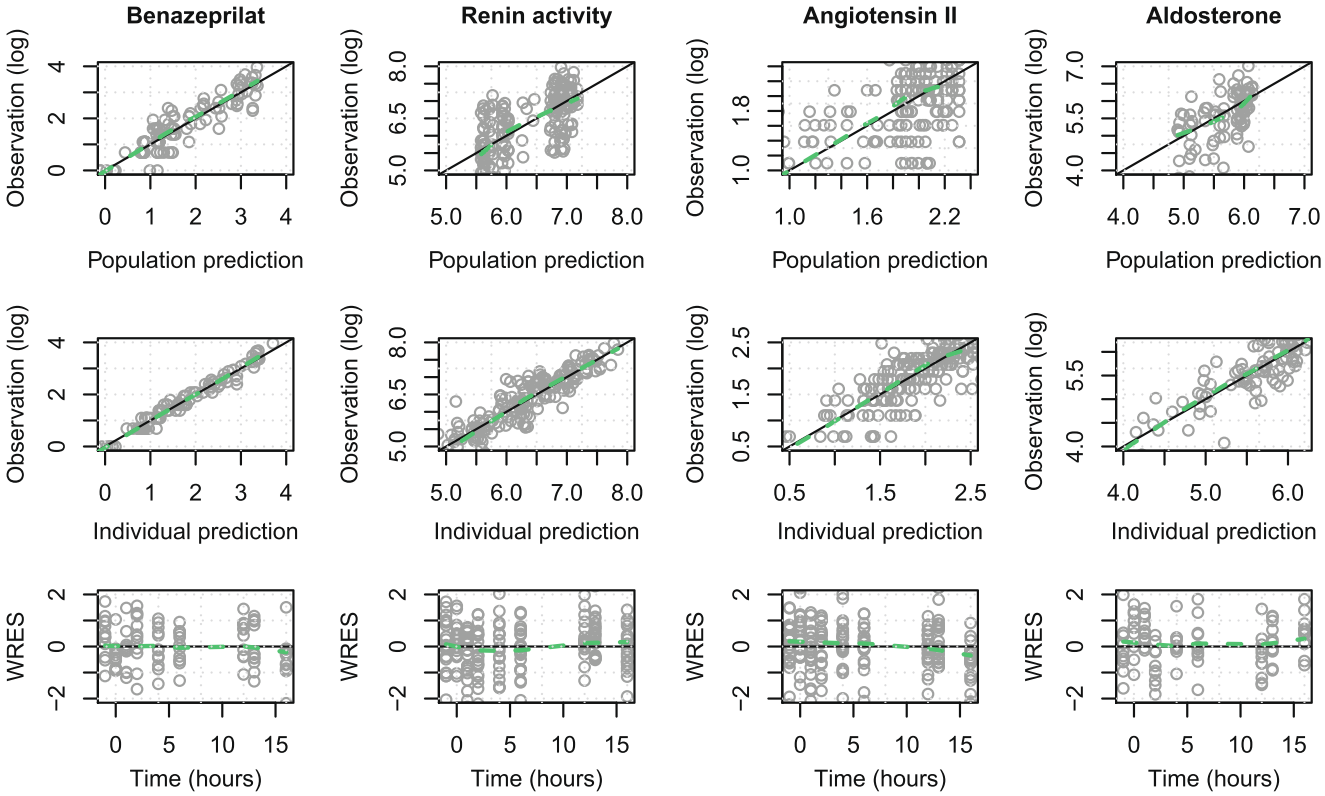

Fig. 4 Standard goodness-of-fit diagnostics. Scatter plot of population (*top pane*) and individual predictions (*middle pane*) *vs.* observations (*log scale*), and weighted residuals (*bottom pane*, WRES) of population predictions. From *left* to *right*: Benazeprilat, RA, AII, and ALD. *Solid black line*: identity line. *Dashed green line*: regression line. For WRES, the x-axis represents time after dosing (hours). Note: Population predictions are estimates of the median plasma concentration (benazeprilat, AII, and ALD), or enzyme activity (*RA*). A suitable model has the following features: (*i*) the line of identity is aligned with the regression line (for both individual and population predictions), while (*ii*) the residues (differences between observations and predictions) are centered on a mean value of 0, with (*iii*) a homogeneous dispersion around the mean.

2. *Modeling of angiotensin II data*

Total benazeprilat concentrations were found to mirror well the time-variations of observed AII, such that benazeprilat concentration-time data predicted from Eqs. 2 to 5, could be used as the driving force in an immediate response submodel (Eqs. 11 and 12):

$$E_1(C_{ij}) = 1 - \left(\frac{I_{max,i\ (AII)} \cdot C_{ij}^{\gamma_{i(AII)}}}{IC_{50,i(AII)}^{\gamma_{i(AII)}} + C_{ij}^{\gamma_{i(AII)}}} \right) \tag{11}$$

$$AII(t_{ij}) = f(t_{ij})_{AII} . E_1(C_{ij}) \tag{12}$$

Where $AII(t_{ij})$ is the predicted AII level (pg/ml) at time t_{ij} in a benazepril-treated individual, $f(t_{ij})_{AII}$ is the predicted AII placebo value (pg/ml) at time t_{ij} for that individual i, $E_1(C_{ij})$ is the inhibition function that depends on predicted total benazeprilat concentrations C_{ij} (ng/ml) (Eqs. 2 to 5), $I_{max,i\ (AII)}$ is the maximal inhibition of AII production, $IC_{50,i\ (AII)}$ is the total benazeprilat concentration (ng/ml) that produces half of the maximum inhibition, and $\gamma_{i\ (AII)}$ is the Hill coefficient of the AII_{ij} *vs.* C_{ij} effect curve.

3. *Modeling of renin activity data*

Subsequently, in an attempt to quantify the drug-induced counter-regulation of RA, the differences between predicted AII concentrations during placebo treatment and those at corresponding times after benazepril administration (Δ_{ij}) were used in a 3-parameter sigmoid E_{max} submodel, as follows (Eqs. 13 and 14):

$$E_2(\Delta_{ij}) = 1 + \left(\frac{E_{max,i\ (RA)} \cdot \Delta_{ij}^{\gamma_{i(RA)}}}{EC_{50,i(RA)}^{\gamma_{i(RA)}} + \Delta_{ij}^{\gamma_{i(RA)}}} \right) \tag{13}$$

$$RA(t_{ij}) = f(t_{ij})_{RA} . E_2(\Delta_{ij}) \tag{14}$$

Where $RA(t_{ij})$ is the predicted RA level (pg/ml.h^{-1}) at time t_{ij} in a benazepril-treated individual, $f(t_{ij})_{RA}$ is the predicted RA placebo value (pg/ml.h^{-1}) at time t_{ij} for that individual i, $E_2(\Delta_{ij})$ is the stimulation function that depends on Δ_{ij}, $E_{max,i\ (RA)}$ represents the maximum

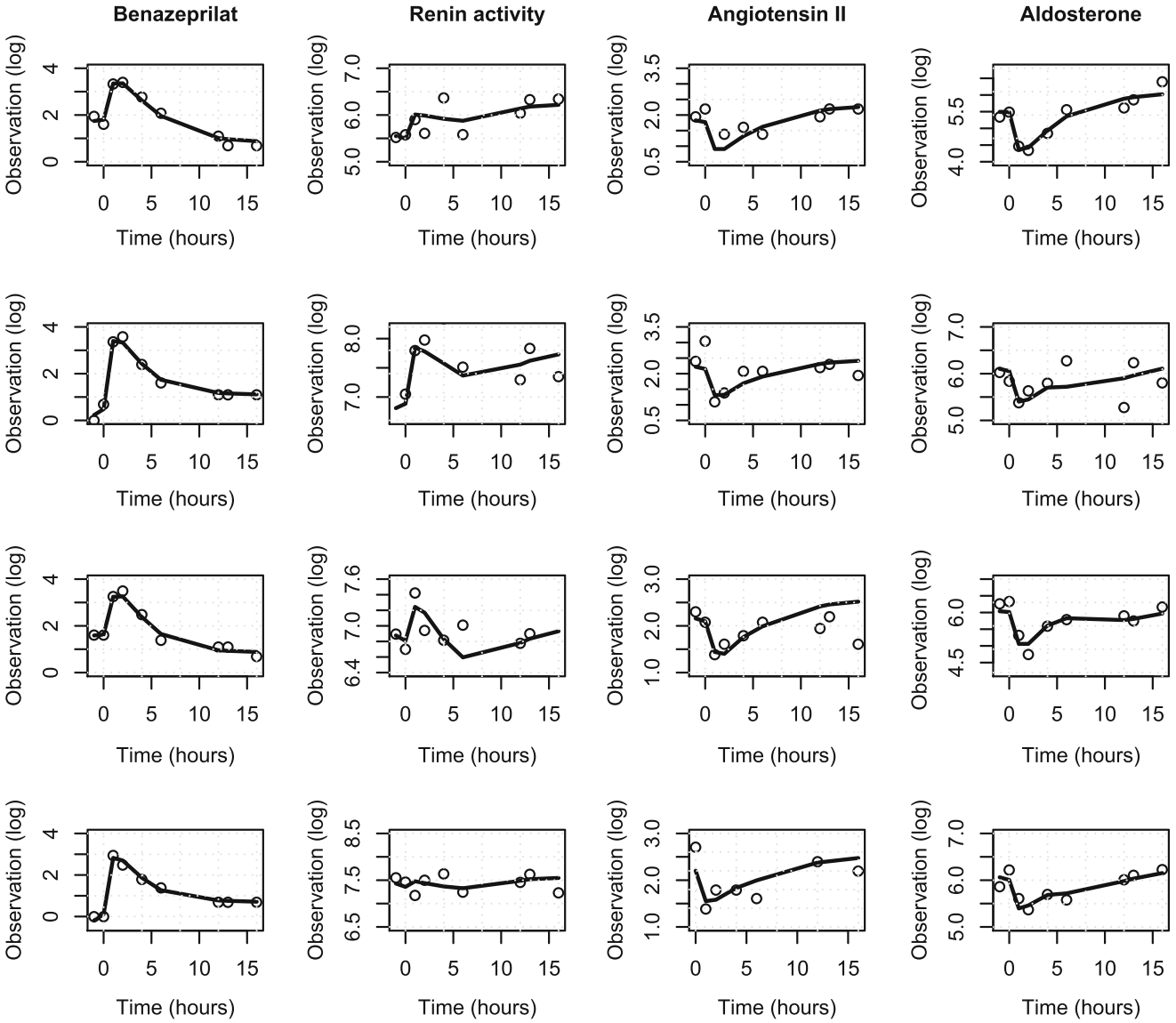

Fig. 5 Individual predictions of benazeprilat disposition and effect on the systemic RAAS. Scatter plot of observed (*open circles*, *log scale*) and predicted (continuous *black line*) individual data *vs.* time after dosing (hour) based on empirical Bayes estimates. Out of clarity only a subset of 4 individuals per endpoint are represented herein (one per row). From *left* to *right*: benazeprilat, RA, AII, and ALD. The full model was able to describe the time-variant changes of the experimental data with high accuracy, as shown by the good agreement between observed and predicted data.

stimulatory effect of Δ_{ij} on renin, $EC_{50,i\ (RA)}$ is the difference in AII (pg/ml) between placebo and benazepril-treated dogs for achieving 50% of the maximal stimulation of RA, and $\gamma_{i(RA)}$ is the Hill coefficient of the RA_{ij} *vs.* Δ_{ij} effect curve.

4. *Modeling of aldosterone data*

The reduction of AII following ACE inhibition therapy was finally used as the driving force to predict ALD time-variations in the following empirical submodel (Eqs. 15 and 16):

$$E_3(\Delta_{ij}) = 1 - \left(\frac{I_{max,i\ (ALD)} \cdot \Delta_{ij}^{\gamma_{i(ALD)}}}{IC_{50,i(ALD)}^{\gamma_{i(ALD)}} + \Delta_{ij}^{\gamma_{i(ALD)}}} \right) \quad (15)$$

$$ALD(t_{ij}) = f(t_{ij})_{ALD} \cdot E_3(\Delta_{ij}) \quad (16)$$

Where $ALD(t_{ij})$ is the predicted ALD level (pg/ml) at time t_{ij} in a benazepril-treated individual, $f(t_{ij})_{ALD}$ is the predicted ALD placebo value (pg/ml) at time t_{ij} for that individual i, $E_3(\Delta_{ij})$ is the inhibition function that depends on predicted Δ_{ij}, $I_{max,i\ (ALD)}$ is the maximal inhibition of ALD production, $IC_{50,i\ (ALD)}$ is the difference in AII (pg/ml) between placebo and benazepril-treated dogs for achieving 50% of the maximal inhibition of ALD, and $\gamma_{i(ALD)}$ is the Hill coefficient of the ALD_{ij} *vs.* Δ_{ij} effect curve.

The final full model, which enabled the simultaneous fit of AII, RA, and ALD data, was found to characterize the

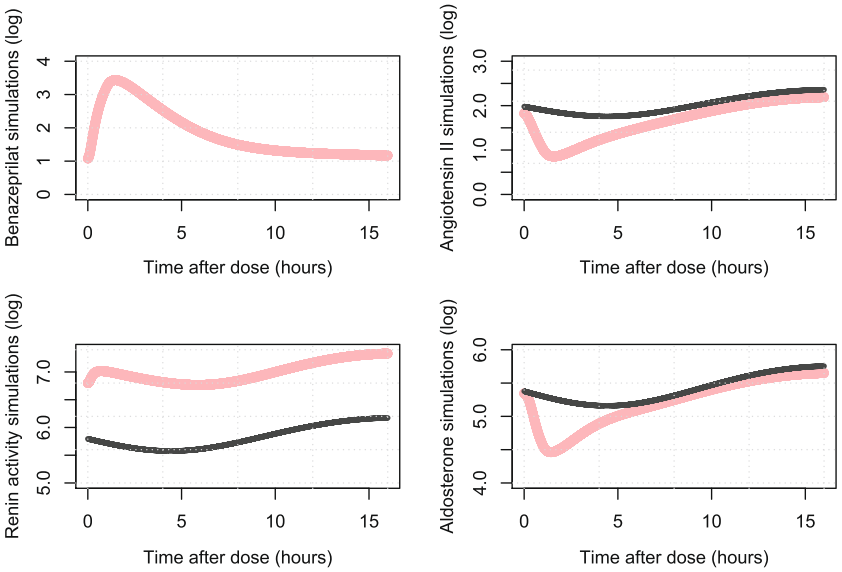

Fig. 6 Simulated pharmacokinetic and pharmacodynamic properties of benazeprilat in healthy beagle dogs fed a low-sodium diet. Benazeprilat (*top left pane*), AII (*top right pane*), RA (*bottom left pane*) and ALD (*bottom right pane*) simulations using final parameter estimates from Tables I, III and IV (step size for the numerical Runge–Kutta integrator: 0.01 h). Continuous *grey line*: simulated time-course profiles in a typical placebo-treated dog, thick continuous *red line*: simulated time-course profiles in a typical benazepril-treated individual (5 mg PO, q24 h). The performance of the full model in reproducing the data can be appreciated by comparing the simulations to the raw observations presented in Figs. 1 and 2.

time-varying changes of the renin-angiotensin aldosterone cascade satisfactorily, as shown by the standard goodness-of-fit diagnostics (Fig. 4), the individual predictions (Fig. 5), and the simulation-based validation diagnostics (Figs. 6, 7, and Supplementary Material). A quasi-proportional error model (*i.e.* additive error in the log domain) was used to

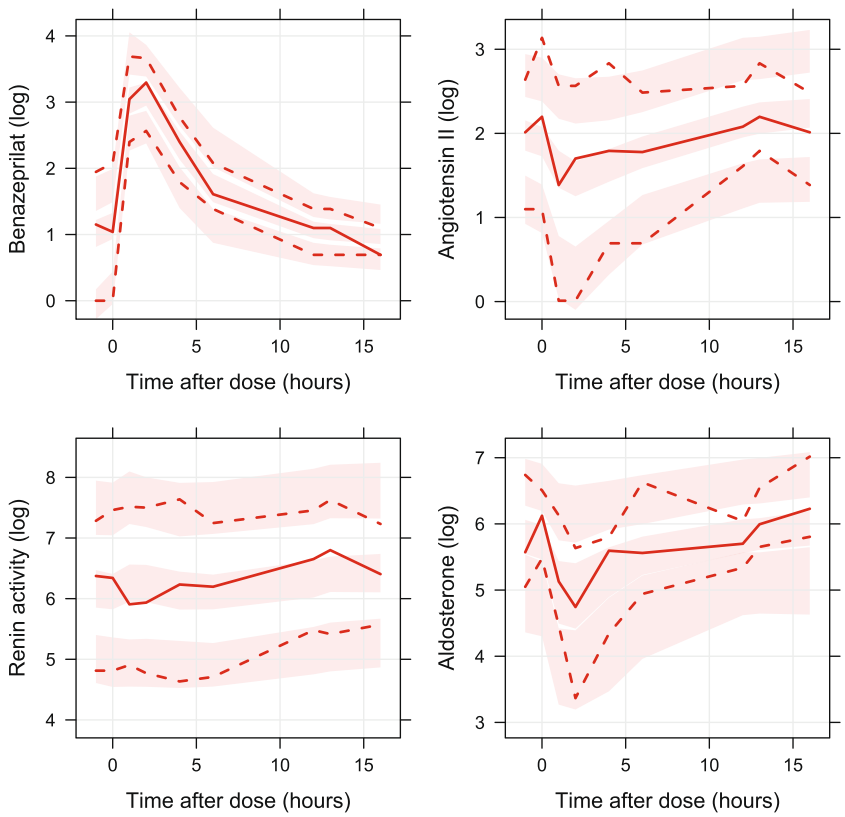

Fig. 7 Visual predictive checks of the full pharmacokinetic/pharmacodynamic model. Visual predictive checks of benazeprilat pharmacokinetic (*top left pane*) and action on AII (*top right pane*), RA (*bottom left pane*), and ALD (*bottom right pane*) generated from 1000 Monte Carlo simulations. Solid and *dashed red line*: median, 5th and 95th percentiles of the observed data. *Middle red shaded area*: 80% confidence interval of the simulated median. *Lower and upper red shaded areas*: 80% confidence interval of the simulated 5th and 95th percentiles. The full PK/PD model was able to capture the time-varying changes of benazeprilat, RA, AII, and ALD reasonably well, as shown by the good agreement between observed and model-predicted percentiles.

Table I Parameter Estimates of the Pharmacokinetic Model

	Point estimate	Unit	RSE (%)	BSV
T_{inf}	1:02	h:min	11	0.33
ka	2.2	h^{-1}	19	0.10
k_{10}	0.56	h^{-1}	12	0.20
k_1	0.011	$nM^{-1}.h^{-1}$	32	–
k_2	0.010	h^{-1}	7	–
BS	0.025	nM	10	–
V_c/F	6.3	l/kg	15	0.10
Sex on V_c/F	1.4	–	9	–

Abbreviations. T_{inf} duration of the hypothetical infusion into the depot compartment, *ka* first-order rate constant representing the absorption of benazepril into the central compartment and its *in vivo* conversion to benazeprilat, k_{10} 1st-order rate constant of benazeprilat elimination from the central compartment, k_1 and k_2 2nd and 1st-order rate constants of association/dissociation of the benazeprilat-ACE complex, *BS* maximal binding capacity to circulating ACE, V_c/F apparent volume of distribution of benazeprilat, *Sex on* V_c/F Multiplicative effect of sex (male) on benazeprilat apparent volume of distribution. *RSE* relative standard error, *BSV* between-subject variability (expressed as standard deviation of the random effect)

BSV was tentatively introduced on k_1, k_2, and *BS* parameters of the pharmacokinetic model, but it was estimated to be rather small, and therefore fixed to 0

account for the residual noise in the measurement of RA, AII, and ALD. Population parameter estimates (including between-subject variability), and relative standard errors are listed in Tables III and IV. Estimates of residual errors (CV%) from the mathematical models were 32%, 42%, and 40% for RA, AII, and ALD, respectively. The precision of the final model parameters was considered satisfactory (RSE < 35% for most of the parameters).

According to the PK/PD model, the level of benazeprilat that produces 50% of the maximal inhibition of AII would be 17.9 ng/ml (Table IV). Benazeprilat peak concentrations (31 ng/ml) caused on average a 2.8-fold reduction of AII, with a subsequent 2.6-fold increase in RA, and a 2.3-fold decrease in ALD compared with placebo (Fig. 6). Differences in AII between placebo and benazepril-treated dogs for achieving half of the maximal stimulation of RA, and half of the maximum inhibition of ALD were estimated to be rather small (1.0 and 3.6 pg/ml for RA and ALD, respectively). This suggests that modest changes in AII can trigger substantial variations in RA and ALD, which is in agreement with the estimated large Hill coefficients (approximately 2 to 3), reflective of a steep concentration-effect curve. Lastly, bodyweight and sex were not found to have a significant influence on the parameter estimates of the pharmacodynamic model.

Table II Comparison of Objective Function Value (OFV) for Statistical Testing of the Zero-Amplitude Hypothesis

	Renin activity (RA)	Angiotensin II (AII)	Aldosterone (ALD)
OFV (straight line)	−18.2	−61.9	13.5
OFV (cosine model)	−57.5	−101.9	−25.2
Difference in OFV	−39.2	−40.0	−38.7
p-value	<0.01	<0.01	<0.01

For rhythm detection, a *p*-value was derived from the difference in OFV between the fit of a constant mean, and that of a cosine function. A periodic rhythm was considered as statistically significant for a drop in OFV > 5.9 (for a risk level α: 0.05). Model estimates of the amplitudes can be found in Table III

DISCUSSION

Although modulation of the renin cascade by ACE inhibitors is the mainstay of treatment of cardiovascular disorders in small animals, no detailed information about the temporal relation of benazeprilat to circulating RAAS peptides is currently available in the veterinary literature. The objective of this study was to provide a comprehensive description of the effect of benazeprilat on the dynamics of the systemic renin-angiotensin cascade in dogs, using modeling and simulation techniques. MB modeling approaches heighten the understanding of specific mechanisms underlying the drug-effect relationship in a specific biological system (cell, tissue, animal, or animal sub-population). Specifically, a MB PK/PD model that includes the periodic nature of RA, AII, and ALD during placebo treatment and the subsequent changes in dynamics following inhibition of ACE was developed.

Benazeprilat Disposition Kinetics and Effect on Circulating RAAS Peptides

The converting enzyme can be found in a soluble (circulating) form, but also in tissues where it binds to the plasma membrane of vascular endotheliums (22). The soluble form of ACE originates from the membrane-bound form by proteolytic cleavage (24). In our mathematical representation, benazeprilat data were derived from a nonlinear binding (TMDD) model, including a reversible, saturable and specific binding to circulating ACE. Levy (25) was the first to classify certain molecules as having this unique feature by which capacity-limited and high-affinity binding to a target influences the pharmacokinetics of a drug. A more complex pharmacokinetic model, taking into account distribution to tissular ACE was tested, but not supported by the data. The fall of benazeprilat concentrations following absorption should be interpreted as an elimination phase (driven by k_{10}), which controls drug accumulation and time to reach equilibrium (steady state) (10). This equilibrium is commonly attained after a delay of 3 to 5 times the half-life of elimination (26). Thus, for any drug having an elimination half-life of less than 2 h (*e.g.* benazeprilat), steady state conditions are met after the first daily administration. Parameter estimates of the final pharmacokinetic model indicate that benazeprilat has a large apparent volume of distribution (6.3 l/kg), and a high

Table III Parameter Estimates from the Modeling of the Placebo Data

		Point estimate	Unit	RSE (%)	BSV
Angiotensin II (AII)	$M_{(AII)}$	8.2	pg/ml	10	0.35
	$A_{(AII)}$	2.4 (29)	pg/ml (%)	14	–
	$\psi_{(AII)}$	23:20	h:min	16	0.55
Renin activity (RA)	$M_{(RA)}$	372	$pg/ml.h^{-1}$	15	0.56
	$A_{(RA)}$	108 (29)	$pg/ml.h^{-1}$ (%)	14	–
	$\psi_{(RA)}$	23:20	h:min	16	0.55
Aldosterone (ALD)	$M_{(ALD)}$	245	pg/ml	16	0.57
	$A_{(ALD)}$	71 (29)	pg/ml (%)	14	–
	$\psi_{(ALD)}$	23:20	h:min	16	0.55

Abbreviations: $M_{(AII,\ RA,\ ALD)}$ mesor (daily average of rhythm) of AII, RA, or ALD, $A_{(AII,\ RA,\ ALD)}$ and $\psi_{(AII,\ RA,\ ALD)}$ amplitude and acrophase (time of peak) of the cosine function that describes time-varying changes in AII, RA, or ALD. *RSE* relative standard error, *BSV* between-subject variability (expressed as standard deviation of the random effect). Amplitudes are presented in absolute and relative units (using the mesor value as reference). Data from the various variables were fitted simultaneously, using the periodic nature of RA to estimate the acrophase and the relative amplitude of downstream biomarkers AII and ALD

Note on BSV: for the sake of parsimoniousity and to avoid model overparameterization, BSV was only introduced on the most relevant pharmacodynamic parameters. For modeling of the placebo data:

- The amplitude of the cosine functions was expressed relative to the mesor value (as %): therefore BSV was only estimated for the mesor RA, AII, and ALD, not the amplitude;

- The acrophase RA, AII, and ALD was set to a same typical value, such that BSV could be distributed across the 3 biomarkers using the same eta term

apparent systemic clearance (3.5 $l.h^{-1}$/kg), associated with a rapid elimination constant (0.56 h^{-1}). These figures are in agreement with previous investigations from Toutain *et al.* (22) in dogs, using a more complex physiological-based kinetics model (4.9 l/kg and 5.5 $l.h^{-1}$/kg for V_c/F and Cl/F, respectively). In addition, the slow dissociation of benazeprilat from its target (k_2: 0.01 h^{-1}) unveils that the terminal phase of benazeprilat disposition is driven by unbinding processes, rather than elimination from the central compartment. Compared with the *in vivo* dissociation constant (k_d) reported by Toutain *et al.* (22) (3.9 nM), the estimated k_d (k_2/k_1) obtained from our model is considered small (ca. 0.9 nM). However, the value from Toutain *et al.* represents the concentration of benazeprilat that produces saturation of half of the entire

Table IV Parameter Estimates of the Mechanism-Based PK/PD Nonlinear Mixed-Effects Model

		Point estimate	Unit	RSE (%)	BSV
Angiotensin II (AII)	$I_{max\ (AII)}$	1	–	§	–
	$IC_{50\ (AII)}$	17.9	ng/ml	27	0.48
	$\gamma_{(AII)}$	1	–	§	–
Renin activity (RA)	$E_{max\ (RA)}$	2.8	–	18	0.40
	$EC_{50\ (RA)}$	1	pg/ml	49	1.20
	$\gamma_{(RA)}$	1.7	–	35	–
Aldosterone (ALD)	$I_{max\ (ALD)}$	0.9	–	2	–
	$IC_{50\ (ALD)}$	3.6	pg/ml	28	0.72
	$\gamma_{(ALD)}$	2.7	–	16	–

Abbreviations. $I_{max\ (AII)}$ maximum inhibition of AII production, $IC_{50\ (AII)}$ benazeprilat concentration that produces half of the maximum inhibition, $\gamma_{(AII)}$ Hill coefficient of the AII *vs.* benazeprilat effect curve, $E_{max\ (RA)}$ maximum stimulatory effect on RA, $EC_{50\ (RA)}$ difference in AII between placebo and benazepril-treated dogs for achieving 50% of the maximal stimulation of RA, $\gamma_{(RA)}$ Hill coefficient of the RA *vs.* AII effect curve, $I_{max\ (ALD)}$ maximum inhibition of ALD production, $IC_{50\ (ALD)}$ difference in AII between placebo and benazepril-treated dogs for achieving 50% of the maximal inhibition of ALD, $\gamma_{(ALD)}$ Hill coefficient of the ALD *vs.* AII effect curve; §: fixed value. RSE: relative standard error; BSV: between-subject variability (expressed as standard deviation of the random effect)

Note on BSV: for the sake of parsimoniousity and to avoid model overparameterization, BSV was only introduced on the most relevant pharmacodynamic parameters. For modeling of the drug effect:

- Because only 1 level of dose of benazepril was used in the experiment, the estimated maximum inhibition of AII/ALD and the related $IC_{50\ (AII)}$/ $IC_{50\ (ALD)}$ value were highly correlated, such that BSV was only introduced on the potency terms;

- For similar considerations, BSV was not introduced on the Hill coefficients of the various concentration-response relationships

ACE pool, including the *tissular* form. In contrast, the k_d estimated from our model only accounts for the binding of benazeprilat to *circulating* ACE, which is modest compared with *tissular* ACE. Results from the present research also demonstrate that peptides of the renin-angiotensin cascade oscillate with a circadian periodicity in healthy beagle dogs fed a low-sodium diet (0.05% sodium) at 13:00 h. A cosine model with a fixed 24-h period was found to fit the periodic variations of RA, AII, and ALD well, as suggested by the results of the zero-amplitude hypothesis testing. Renin, AII, and ALD were found to oscillate in parallel over the observation span, with a peak lying around 23:00 h, and a relative amplitude of 29%. Characterization of the time-varying changes in RA, AII and ALD is key to quantifying the modulatory effect of benazepril on the dynamics of the circulating RAAS. Specifically, looking at the simulated profiles of benazeprilat pharmacodynamics in Fig. 6, one understands that the use of a straight line approximation of the mean (instead of a cosine) for modeling of the placebo data would have resulted in overestimating the effect of benazeprilat on AII and ALD, while underestimating its effect on RA. Deeper understanding of circadian rhythms can have a substantial impact on the therapeutic management of RAAS-related diseases by determining the time of drug administration that would optimize efficacy while minimizing the occurrence of adverse effects. This concept, referred to as chronotherapy, has been used for several years in the management of human rheumatoid arthritis, cancer, and cardiovascular diseases (27). In comparison with data from our earlier research in healthy dogs fed a normal-sodium regime (0.5% sodium) (17), the mesor and amplitude value of RA would be almost 4.0 times greater in dogs fed a low sodium diet (0.05% sodium). This consolidates our preliminary findings that dietary sodium interacts with the renin cascade, not only by influencing the tonic (*i.e.* mesor), but also the phasic (*i.e.* amplitude) secretion of renin (*i.e.* the greater the sodium intake, the smaller the mesor and the amplitude of RA).

The modulatory action of benazeprilat on the RAAS was characterized using an integrated mechanism-based PK/PD model, where benazeprilat concentration *vs.* time data served as the driving force for prediction of AII, while RA and ALD were estimated from the difference in AII during placebo and benazepril treatment. Looking at the individual time-course profiles, no substantial time delay was observed between benazeprilat, RA, AII, and ALD dynamics in benazepril treated dogs, which is an indication of a rapid turn-over of RAAS biomarkers. Therefore, the effect of benazeprilat on the RAAS could be described using a combination of immediate response models.

Various PD studies on ACE inhibitors have failed to show a meaningful effect on circulating levels of AII and ALD in dogs. Knowlen *et al.* (28) have reported non-significant differences between pre-dose (367 ± 191 pg/ml) and post-dose (217 ± 173 pg/ml) ALD values after repeated administrations with captopril in 7 CHF dogs. Likewise, oral administrations of enalapril did not produce a significant fall in AII after 3 weeks of treatment in a dog study by Häggström *et al.* (29). In another experiment with enalapril by Koch *et al.* (30) in 8 male beagle dogs, ALD levels were not different from baseline measurements 24 h post-dose. Consistent with our previous investigations (11), our data show that benazepril noticeably influences the dynamics of the systemic RAAS at its recommended dose in dogs (0.25–1 mg/kg PO q24 h), resulting in a substantial reduction of AII and ALD, while increasing RA. In this low-sodium model of RAAS activation benazeprilat peak concentrations triggered on average a 2.8 and 2.3-fold decrease in AII and ALD levels, with a compensatory 2.6-fold increase in RA compared with placebo. The elevation of RA, as a consequence of benazepril-induced interruption of the AII-renin negative feedback loop (31), is commonly used as a surrogate marker of efficacy for monitoring time-dependent RAAS inhibition (32,33). Differences in the duration of effect of benazeprilat on the various RAAS biomarkers are also noteworthy. Simulations from the final PK/PD model suggest that the effect of benazeprilat on AII and ALD lasts between 5 and 10 h, while RA increases above placebo levels throughout the 16-h observation period. The contrast between RA and ALD is in agreement with the estimated $EC_{50\ (RA)}$ (1.0 pg/ml AII *vs.* 3.6 pg/ml for $IC_{50\ (ALD)}$), which indicates that small changes in AII are responsible for marked variations in RA.

Why ACE Activity is not a Reflective Measure of RAAS Suppression

ACE inhibitors have constituted a breakthrough therapeutic option in the management of cardiovascular diseases in human and veterinary patients (8,34). Earlier investigations on the use of benazepril in dogs have established that benazeprilat produces a complete and long-lasting inhibition of ACE. In a study by King *et al.* (35), oral administrations of benazepril (0.25 mg/kg q24 h) were responsible for more than 85% inhibition of ACE during 24 h. In addition, Toutain and Lefebvre (10) have shown that an oral daily dose of 0.125 mg/kg benazepril causes inhibition of the entire systemic ACE pool within 48 h. Our results demonstrate that benazeprilat triggers a marked fall in AII and ALD, but for a much shorter period of time, which is consistent with earlier observations in dog and human patients (11,12,36). According to Van de Wal *et al.* (13), 45% of severe CHF patients experience elevated AII levels independent of serum ACE activity. In individuals with high ACE activity, non-compliance should be considered along with inadequate dose selection as potential explanations. Yet, in patients with low measurable ACE activity, this could be related to the production of AII by up-regulation of ACE independent pathways (37), in response to renin activation and accumulation of AI during short and

long-term use of ACE inhibitors (31). Enzymes other than ACE may contribute to the conversion of AI to AII. Chymase, cathepsin G, tonin and other proteases have been described as alternative pathways of AII production (4). The incomplete reduction of AII observed in our experiment may however be the result of the opposite stimulatory effect of sodium depletion on the RAAS. In that respect, the dose of benazepril used herein might have been insufficiently high to offset the low-sodium-induced activation of the renin cascade.

Our findings on ALD are in agreement with earlier reports from the veterinary ((28); Koch *et al.* 1994) and human literature (12,38). Because AII is a known driver of ALD biosynthesis (39), the partial suppression of AII in ACE inhibitor-treated dogs may account for the insufficient suppression of systemic ALD levels. Moreover, the possibility of an enhanced sensitivity of the adrenal glands to AII during chronic ACE inhibitor usage cannot be discarded (12). Finally, like all ACE inhibitors, benazeprilat has the potential to induce natriuresis and potassium retention, which can further stimulate secretion of ALD from the adrenals.

Clinical Implications

In humans, the degree of activation of the renin-angiotensin aldosterone cascade is related to the severity of heart failure (40,41). In this population of patients, AII concentrations vary from less than 10 pg/ml in mild cases of CHF, to 70 pg/ml in seriously affected individuals (13). AII is viewed as a primary determinant of end-organ damage (4), while ALD is known to worsen AII tissue-damaging properties (42). Thereof, elevated exposure to AII and ALD has been associated with a poor prognosis in multiple case studies (4,43). Swedberg *et al.* (40) have found a positive correlation between mortality and levels of AII ($p<0.05$) and ALD ($p<0.003$) in a group of severe CHF patients. More recently, a 12 months follow-up study showed that AII was a significant predictor of death or new heart failure episodes in patients with left ventricular dysfunction (4). Likewise, high ALD concentrations were found to be a predictor of increased mortality risk that provides complementary prognostic value in a prospective cohort experiment of 294 patients with CHF of any cause and severity (5).

Compared with the depth of data from the human literature, only limited information on the relation of AII and ALD to a morbidity and mortality risk is presently available in dogs. Knowlen *et al.* (28) have established a direct relationship between ALD and the clinical status of dogs suffering from heart failure. Results from Bernay *et al.* (44) in a multicenter prospective trial indicate that ALD receptor antagonism decreases the risk of cardiac death, euthanasia, or severe worsening in dogs with moderate to severe CVHD. Ovaert *et al.* (45) suggest that patients with elevated AII and ALD could benefit from additional therapy with AII receptor blockers (ARBs), or ARAs. However, ALD escape has also been reported during long-term use of ARBs and ARAs (46,47). In a study by Naruse *et al.* (46), ALD increased above pre-treatment levels after 8 weeks of ARB administration, causing end-organ damage and left ventricular hypertrophy in rodents. In addition, results from the RALES Neurohormonal Substudy (47) showed a significant increase in AII and ALD over time (p: 0.003 and p: 0.001, respectively) in spironolactone-treated CHF patients.

In the BENCH Study (8), the mean survival time of benazepril-treated dogs with mild to moderate CHF was improved by a factor of 2.7, as compared with the placebo group (428 *vs.* 158 days). A significant gain in exercise tolerance and clinical condition was also reported after 28 days of treatment. The favorable outcome of most CHF canine patients under ACE inhibition therapy, despite a potential incomplete reduction in AII and ALD, suggests that ACE inhibitors exert additional beneficial effects than AII suppression in the course of heart disease (34,48). As pointed out by Brown and Vaughan (49), inhibition of bradykinin degradation, which results in a subsequent gain in left ventricular relaxation and systolic dysfunction, may account for the clinical effectiveness of ACE inhibitors. Along with its effect on ACE inhibition and bradykinin degradation, the blood pressure-lowering action of benazepril could also drive part of the reported clinical efficacy. Cardiac remodeling is a known deleterious consequence of arterial hypertension (50), and benazepril (2 mg/kg q24 h PO, for 2 weeks) has been shown to reduce blood pressure significantly ($p<0.05$) in a dog model of renal hypertension (51).

Limitations

In an experiment by Kjolby *et al.* (52) in dogs fed a low-sodium regime (0.5 mmol/kg/day), AII and ALD increased by 140 and 1800%. Results from our earlier research (53) also indicated a 8 to 10 fold rise in urinary ALD in 6 healthy beagle dogs fed a low-salt diet (0.05% sodium) for 10 days. While sodium restriction is a powerful stimulant of the renin-angiotensin cascade, a detailed description of AII and ALD levels in dogs suffering from CHF is currently missing. In that respect, the effect of benazeprilat on circulating RAAS peptides may have been hampered by the too strong stimulatory effect of sodium depletion, such that, one could expect greater blockade of RAAS with benazepril in heart diseased dogs. Furthermore, the use of several increasing doses of benazepril (instead of 1) would have provided more accuracy on the estimated model parameters. To better characterize the relationship between ACE inhibition, AII and ALD, measurement of ACE activity would have been necessary. However, collecting these extra samples would have resulted in exceeding the volume of withdrawn blood authorized in the aforementioned Swiss permit. Finally, the non-significance of some covariate relationships (*e.g.* bodyweight on parameters of the

pharmacokinetic model) should be interpreted with caution given the low statistical power related to the small size of the study.

CONCLUSION

To conclude, we have developed an integrated PK/PD model that efficiently captures the disposition kinetics of benazeprilat, as well as the time-varying changes of systemic renin-angiotensin aldosterone biomarkers without, and with ACE inhibition therapy. This mechanistic representation provides a quantitative framework for better understanding the effect of ACE inhibition on the RAAS.

Our data show that benazeprilat noticeably influences the dynamics of the renin-angiotensin aldosterone cascade in dogs, resulting in a marked but transitory decrease in AII and ALD, while increasing RA all over the observation span. The effect of ACE inhibition on AII and ALD may be one of the drivers of improved survival and quality of life in benazepril-treated dogs. To investigate this hypothesis further, additional efforts should be directed towards profiling of systemic RAAS peptides in symptomatic CHF canine patients.

ACKNOWLEDGMENTS AND DISCLOSURES

These investigations were conducted at the Centre de Recherche Sante Animale SA (CRA) of Novartis Animal Health, located in St-Aubin, Switzerland.

With the exception of Prof. Meindert Danhof, the authors of the manuscript are Novartis employees. The experiments were supported by Novartis Animal Health, Basel, Switzerland.

REFERENCES

1. Atkins C, Bonagura J, Ettinger S, Fox P, Gordon S, Haggstrom J, *et al.* Guidelines for the diagnosis and treatment of canine chronic valvular heart disease. J Vet Intern Med. 2009;23(6):1142–50.
2. Guglielmini C. Cardiovascular diseases in the ageing dog: diagnostic and therapeutic problems. Vet Res Commun. 2003;27(1):555–60.
3. Sayer MB, Atkins CE, Fujii Y, Adams AK, DeFrancesco TC, Keene BW. Acute effect of pimobendan and furosemide on the circulating renin-angiotensin-aldosterone system in healthy dogs. J Vet Intern Med. 2009;23(5):1003–6.
4. Roig E, Perez-Villa F, Morales M, Jiménez W, Orús J, Heras M, *et al.* Clinical implications of increased plasma angiotensin II despite ACE inhibitor therapy in patients with congestive heart failure. Eur Heart J. 2000;21(1):53–7.
5. Güder G, Bauersachs J, Frantz S, Weismann D, Allolio B, Ertl G, *et al.* Complementary and incremental mortality risk prediction by cortisol and aldosterone in chronic heart failure. Circulation. 2007;115(13):1754–61.
6. Tan LB, Jalil JE, Pick R, Janicki JS, Weber KT. Cardiac myocyte necrosis induced by angiotensin II. Circ Res. 1991;69(5):1185–95.
7. Shimizu M, Tanaka R, Fukuyama T, Aoki R, Orito K, Yamane Y. Cardiac remodeling and angiotensin II-forming enzyme activity of the left ventricle in hamsters with chronic pressure overload induced by ascending aortic stenosis. J Vet Med Sci. 2006;68(3):271–6.
8. BENCH (BENazepril in Canine Heart disease) Study Group. The effect of benazepril on survival times and clinical signs of dogs with congestive heart failure: Results of a multicenter, prospective, randomized, double-blinded, placebo-controlled, long-term clinical trial. J Vet Cardiol. 1999;1(1):7–18.
9. Webb R. Benazepril. Cardiovasc Drug Rev. 1990;8(2):89–104.
10. Toutain PL, Lefebvre HP. Pharmacokinetics and pharmacokinetic/pharmacodynamic relationships for angiotensin-converting enzyme inhibitors. J Vet Pharmacol Ther. 2004;27(6):515–25.
11. Mochel JP, Peyrou M, Fink M, Strehlau G, Mohamed R, Giraudel JM, *et al.* Capturing the dynamics of systemic Renin-Angiotensin-Aldosterone System (RAAS) peptides heightens the understanding of the effect of benazepril in dogs. J Vet Pharmacol Ther. 2013;36(2):174–80.
12. Lijnen P, Staessen J, Fagard R, Amery A. Increase in plasma aldosterone during prolonged captopril treatment. Am J Cardiol. 1982;49(6):1561–3.
13. Van de Wal RM, Plokker HW, Lok DJ, Boomsma F, van der Horst FA, van Veldhuisen DJ, *et al.* Determinants of increased angiotensin II levels in severe chronic heart failure patients despite ACE inhibition. Int J Cardiol. 2006;106(3):367–72.
14. Sisson DD. Neuroendocrine evaluation of cardiac disease. Vet Clin North Am Small Anim Pract. 2004;34(5):1105–26.
15. Muller AF, Manning EL, Riondel AM. Influence of position and activity on the secretion of aldosterone. Lancet. 1958;1(7023):711–3.
16. Mochel JP, Fink M, Peyrou M, Desevaux C, Deurinck M, Giraudel JM, *et al.* Chronobiology of the renin-angiotensin-aldosterone system in dogs: relation to blood pressure and renal physiology. Chronobiol Int. 2013;30(9):1144–59.
17. Mochel JP, Fink M, Bon C, Peyrou M, Bieth B, Desevaux C, *et al.* Influence of feeding schedules on the chronobiology of renin activity, urinary electrolytes and blood pressure in dogs. Chronobiol Int. 2014;31(5):715–30.
18. Sheiner LB, Ludden TM. Population pharmacokinetics/dynamics. Annu Rev Pharmacol Toxicol. 1992;32:185–209.
19. Lindbom L, Ribbing J, Jonsson EN. Perl-speaks-NONMEM (PsN)—A Perl module for NONMEM related programming. Comput Methods Programs Biomed. 2004;75:85–94.
20. Jonsson EN, Karlsson MO. Xpose—An S-PLUS based population pharmacokinetic/pharmacodynamic model building aid for NONMEM. Comput Methods Programs Biomed. 1999;58:51–64.
21. Lees KR, Kelman AW, Reid JL, Whiting B. Pharmacokinetics of an ACE inhibitor, S-9780, in man: evidence of tissue binding. J Pharmacokinet Biopharm. 1989;17(5):529–50.
22. Toutain PL, Lefebvre HP, King JN. Benazeprilat disposition and effect in dogs revisited with a pharmacokinetic/pharmacodynamic modeling approach. J Pharmacol Exp Ther. 2000;292(3):1087–93.
23. Picard-Hagen N, Gayrard V, Alvinerie M, Smeyers H, Ricou R, Bousquet-Melou A, *et al.* A nonlabeled method to evaluate cortisol production rate by modeling plasma CBG-free cortisol disposition. Am J Physiol Endocrinol Metab. 2001;281(5):E946–56.
24. Oppong SY, Hooper NM. Characterization of a secretase activity which releases angiotensin-converting enzyme from the membrane. Biochem J. 1993;292(Pt 2):597–603.
25. Levy G. Pharmacologic target-mediated drug disposition. Clin Pharmacol Ther. 1994;56(3):248–52.
26. Toutain PL, Bousquet-Melou A. Plasma terminal half-life. J Vet Pharmacol Ther. 2004;27(6):427–39.
27. Nicholls MG, Richards AM, Crozier IG, Espiner EA, Ikram H. Cardiac natriuretic peptides in heart failure. Ann Med. 1993;25(6):503–5.

28. Knowlen GG, Kittleson MD, Nachreiner RF, Eyster GE. Comparison of plasma aldosterone concentration among clinical status groups of dogs with chronic heart failure. J Am Vet Med Assoc. 1983;183(9):991–6.
29. Häggström J, Hansson K, Karlberg BE, Kvart C, Madej A, Olsson K. Effects of long-term treatment with enalapril or hydralazine on the renin-angiotensin-aldosterone system and fluid balance in dogs with naturally acquired mitral valve regurgitation. Am J Vet Res. 1996;57 (11):1645–52.
30. Koch J, Pedersen HD, Jensen AL, Flagstad A, Poulsen K, Bie P. Short term effects of acute inhibition of the angiotensin-converting enzyme on the renin-angiotensin system and plasma atrial natriuretic peptide in healthy dogs fed a low-sodium diet versus a normal-sodium diet. Zentralbl Veterinarmed A. 1994;41(2):121–7.
31. Geary KM, Hunt MK, Peach MJ, Gomez RA, Carey RM. Effects of angiotensin converting enzyme inhibition, sodium depletion, calcium, isoproterenol, and angiotensin II on renin secretion by individual renocortical cells. Endocrinology. 1992;131(4):1588–94.
32. Azizi M, Bissery A, Peyrard S, Guyene TT, Ozoux ML, Floch A, *et al.* Pharmacokinetics and pharmacodynamics of the vasopeptidase inhibitor AVE7688 in humans. Clin Pharmacol Ther. 2006;17(1):13–8.
33. Hong Y, Dingemanse J, Mager DE. Pharmacokinetic/pharmacodynamic modeling of renin biomarkers in subjects treated with the renin inhibitor aliskiren. Clin Pharmacol. 2008;84(1):136–43.
34. Pfeffer MA, Braunwald E, Moyé LA, Basta L, Brown Jr EJ, Cuddy TE, *et al.* Effect of captopril on mortality and morbidity in patients with left ventricular dysfunction after myocardial infarction. Results of the survival and ventricular enlargement trial. The SAVE Investigators. N Engl J Med. 1992;327(10):669–77.
35. King JN, Mauron C, Kaiser G. Pharmacokinetics of the active metabolite of benazepril, benazeprilat, and inhibition of plasma angiotensin-converting enzyme activity after single and repeated administrations to dogs. Am J Vet Res. 1995;56(12):1620–8.
36. Jorde UP, Vittorio T, Katz SD, Colombo PC, Latif F, Le Jemtel TH. Elevated plasma aldosterone levels despite complete inhibition of the vascular angiotensin-converting enzyme in chronic heart failure. Circulation. 2002;106(9):1055–7.
37. Fyhrquist F, Saijonmaa O. Renin-angiotensin system revisited. J Intern Med. 2008;264(3):224–36.
38. Cleland JG, Dargie HJ, Robertson JI. Angiotensin converting enzyme inhibition in heart failure. Br J Clin Pharmacol. 1984;18 Suppl 2:157S–60.
39. McCaa RE, Guyton AC, Young DB, McCaa CS. Role of angiotensin II in the regulation of aldosterone biosynthesis. Adv Exp Med Biol. 1980;130:227–55.
40. Swedberg K, Eneroth P, Kjekshus J, Wilhelmsen L. Hormones regulating cardiovascular function in patients with severe congestive heart failure and their relation to mortality. CONSENSUS Trial Study Group. Circulation. 1990;82(5):1730–6.
41. MacFadyen RJ, Lee AF, Morton JJ, Pringle SD, Struthers AD. How often are angiotensin II and aldosterone concentrations raised during chronic ACE inhibitor treatment in cardiac failure? Heart. 1999;82 (1):57–61.
42. Rocha R, Chander PN, Zuckerman A, Stier CT Jr. Role of aldosterone in renal vascular injury in stroke-prone hypertensive rats. Hypertension. 1999;33(1 Pt 2):232–7.
43. Latini R, Masson S, Anand I, Salio M, Hester A, Judd D, *et al.* The comparative prognostic value of plasma neurohormones at baseline in patients with heart failure enrolled in Val-HeFT. Eur Heart J. 2004;25(4):292–9.
44. Bernay F, Bland JM, Häggström J, Baduel L, Combes B, Lopez A, Kaltsatos V. Efficacy of spironolactone on survival in dogs with naturally occurring mitral regurgitation caused by myxomatous mitral valve disease. J Vet Intern Med. 2010;24(2):331–41.
45. Ovaert P, Elliott J, Bernay F, Guillot E, Bardon T. Aldosterone receptor antagonists: how cardiovascular actions may explain their beneficial effects in heart failure. J Vet Pharmacol Ther. 2010;33(2):109–17.
46. Naruse M, Tanabe A, Sato A, Takagi S, Tsuchiya K, Imaki T, *et al.* Aldosterone breakthrough during angiotensin II receptor antagonist therapy in stroke-prone spontaneously hypertensive rats. Hypertension. 2002;40(1):28–33.
47. Rousseau MF, Gurné O, Duprez D, Van Mieghem W, Robert A, Ahn S, *et al.* Beneficial neurohormonal profile of spironolactone in severe congestive heart failure: results from the RALES neurohormonal substudy. J Am Coll Cardiol. 2002;40(9):1596–601.
48. The CONSENSUS Trial Study Group. Effects of enalapril on mortality in severe congestive heart failure. Results of the Cooperative North Scandinavian Enalapril Survival Study (CONSENSUS). N Engl J Med. 1987;316(23):1429–35.
49. Brown NJ, Vaughan DE. Angiotensin-converting enzyme inhibitors. Circulation. 1998;97(14):1411–20.
50. Azibani F, Fazal L, Chatziantoniou C, Samuel JL, Delcayre C. Hypertension-induced fibrosis: a balance story. Ann Cardiol Angeiol. 2012;61(3):150–5.
51. Mishina M, Watanabe T. Development of hypertension and effects of benazepril hydrochloride in a canine remnant kidney model of chronic renal failure. J Vet Med Sci. 2008;70(5):455–60.
52. Kjolby MJ, Kompanowska-Jezierska E, Wamberg S, Bie P. Effects of sodium intake on plasma potassium and renin angiotensin aldosterone system in conscious dogs. Acta Physiol Scand. 2005;184(3):225–34.
53. Mochel JP, Fink M. Response to letter from Atkins *et al.* J Vet Pharmacol Ther. 2012;35(5):516–8.